Evidence for logarithmic corrections to the mean-field critical behavior in the weak itinerant ferromagnet Ni_3Al

Anita Semwal and S. N. Kaul*
School of Physics, University of Hyderabad, Central University P.O., Hyderabad 500 046, Andhra Pradesh, India
(Received 12 February 2001; published 15 June 2001)

The results of an elaborate analysis of high-resolution magnetization and ac suceptibility data unambiguously establish the existence of multiplicative logarithmic corrections (MLC) to single power laws in the asymptotic critical region near the ferromagnetic–paramagnetic phase transition in well-characterized polycrystalline Ni_3Al samples. A crossover from this asymptotic critical behavior to the Gaussian fixed point occurs gradually over a fairly wide temperature range outside the critical regime. Accurate determination of the universal amplitude ratio $R_\chi = DB^{\delta-1}\Gamma$, the asymptotic critical exponents β, γ, and δ and the MLC exponents x^-, x^+, and x^0 for spontaneous magnetization, initial susceptibility and the magnetization versus field isotherm at $T=T_C$ (the Curie temperature), respectively, and a detailed comparison between theory and experiment indicate that the weak itinerant ferromagnet Ni_3Al, so far as its asymptotic critical behavior is concerned, is an experimental realization of an *isotropic* $d=3$, $n=3$ ferromagnet in which the interactions between magnetic moments decay with distance (r) as $J(r)\sim 1/r^{(3/2)d}$.

DOI: 10.1103/PhysRevB.64.014417 PACS number(s): 75.40.Cx, 64.60.Fr, 75.30.Kz

I. INTRODUCTION

The theoretical formulations that modify the Stoner mean-field model to include[1] zero-point (quantum) and thermally excited spin fluctuations give a fairly accurate estimate of Curie temperature T_C, closely reproduce the observed temperature dependence of spontaneous magnetization, $M(T,0)$, for $T<T_C$ and Curie-Weiss behavior of susceptibility, $\chi(T)$, for $T>T_C$, and correctly predict a second-order phase transition[2,3] at T_C in weak itinerant-electron ferromagnets. Even though these theories successfully explain a host of other characteristic properties[1,2] of weak itinerant ferromagnets as well, they fail[2,4] to properly describe the *critical* behavior of the systems in question. This inadequacy stems from the fact that the spin fluctuation models[1–4] do not take as satisfactory an account of the *critical* fluctuations of the order parameter and the *correlations* between them as theories of critical phenomena normally do. On the other hand, most of the theories of critical phenomena in magnets consider these systems as consisting of magnetic moments (spins) *localized* at lattice sites and interacting with one another through exchange interactions that are of appreciable strength for the *nearest* neighbors only. Notable exceptions to this rule are the theoretical treatments of (i) Heisenberg-spin system with long-range dipolar[5,6] interactions, (ii) *d-dimensional* spin system with an *isotropic n-component* order parameter, in which *long-range* attractive interactions between spins decay[7] with distance as $J(r)\sim 1/r^{d+\sigma}(\sigma>0)$, and (iii) the spherical model (i.e., $n\to\infty$) version[8] of (ii). Thus the choice of theoretical models applicable to itinerant ferromagnets is restricted to these three only.

Experimental studies of critical behavior of weak itinerant ferromagnets near the ferromagnetic-paramagnetic phase transition have been confined to a few systems only[9–11] and rarely more than two critical exponents have been determined. Such studies have yielded a wide range of values for the critical exponents β, γ, and δ for spontaneous magnetization, $M(T,0)$, initial susceptiblity, $\chi(T)$, and the critical isotherm, $M(T_C,H)$; mean-field and three-dimensional isotropic nearest-neighbor Heisenberg/isotropic dipolar estimates fall within this range. Therefore, the exact nature of the dominant singularity at T_C in weak itinerant ferromagnets has remained a mystery despite some theoretical and experimental effort put in so far to unravel it. Other related, but basic questions that have gone unanswered until now are: (a) Which model forms the most appropriate theoretical description of the critical-point behavior of weak itinerant ferromagnets? and (b) Do weak itinerant-electron ferromagnets fall naturally into one of the known universality classes of critical phenomena or do they form a class of their own?

II. EXPERIMENTAL DETAILS

Extensive high-resolution (50 ppm) magnetization, $M(T,H_{ext})$, measurements were performed on well-characterized[12] *polycrystalline* Ni_3Al samples in external static magnetic fields (H_{ext}) up to 15 kOe over a wide temperature range, 15 K$\leqslant T\leqslant$300 K, embracing the critical region near the ferromagnetic-paramagnetic phase transition. After compensating for the earth's magnetic field, the ''in-phase'' component of ac susceptibility (χ_{ac}) was measured to a relative accuracy of $\sim$10 ppm on samples, coming from the same batch as that used in bulk magnetization measurements, at various *fixed* rms amplitudes (1 mOe$\leqslant H_{ac}\leqslant$100 mOe) and frequencies (18.7 Hz$\leqslant\nu\leqslant$187 Hz) of the ac driving field H_{ac} (applied along the length in the sample plane) in the temperature interval, 10 K$\leqslant T\leqslant$120 K. Considerations such as optimum signal-to-noise ratio and *linear* response to H_{ac} at a given temperature restrict the choice of H_{ac} and ν to 10 mOe and 87 Hz, respectively. The details about the sample preparation and characterization are given elsewhere.[12] The samples used for $M(T,H_{ext})$ and χ_{ac} measurements were spherical (2.5 mm in diameter) and rectangular parallelopiped (dimensions: 40

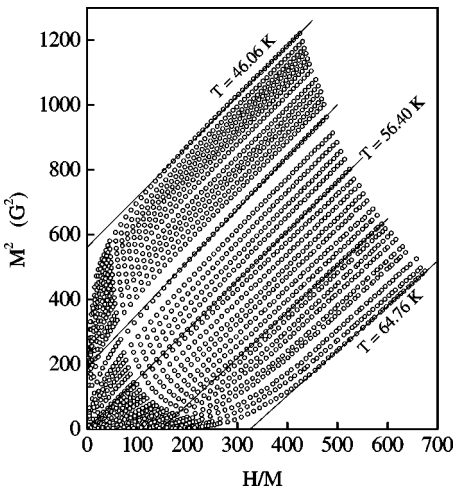

FIG. 1. M^2 vs H/M (Arrott) plot for Ni_3Al in the temperature range T_C-10 K$\lesssim T\lesssim T_C+10$ K.

$\times 2.5\times 0.5$ mm^3) in shape and had undergone annealing at 520°C for 16 days. A detailed analysis of the x-ray diffraction patterns taken on the annealed samples yields[12] the values for the lattice constant and long-range (atomic) order parameter as $a=3.564(2)$ Å and $S=0.55(3)$, respectively. The demagnetizing factor N for the spherical sample was determined from the M-H_{ext} isotherms taken at low fields (-20 Oe$\lesssim$H$_{ext}\lesssim$20 Oe) and temperatures well below the Curie temperature, T_C, whereas for the parallelopiped sample, it was deduced from the relation $\chi^{-1}(T)=\chi_{ac}^{-1}(T)-4\pi N$ using N as a parameter such that at $T=T_C$, $\chi^{-1}(T_C)=0$ as $\chi_{ac}^{-1}(T_C)=4\pi N$. The values of N so estimated are in very good agreement with those calculated from the well-known Osborn formula using the actual sample dimensions. M-H_{ext} isotherms in fields up to 15 kOe and $\chi_{ac}(T)$ were measured at *fixed* (to within ± 5 mK) temperatures $\simeq 25$ mK apart in the temperature interval T_C-2 K$\lesssim T\lesssim T_C+2$ K and at larger intervals outside this temperature range.

III. DATA ANALYSIS

The Arrott $[M(T,H)]^2$ vs $H/M(T,H)$ plot is constructed out of the raw M-H_{ext} isotherms taken in the critical region after correcting the external magnetic field for demagnetization [i.e., $H=H_{ext}-4\pi NM(T,H_{ext})$]. The ''zero-field'' quantities such as spontaneous magnetization, $M(T,0)$, and inverse initial susceptibility, $\chi^{-1}(T)\equiv\chi_{dc}^{-1}(T)$, are computed from the intercept values at different temperatures on the ordinate ($T\lesssim T_C$) and abscissa ($T\gtrsim T_C$) obtained when the *linear* high-field portions of the $[M(T,H)]^2$ vs $H/M(T,H)$ (Arrott) plot isotherms are extrapolated to $H=0$ and $M^2=0$, respectively, as shown in Fig. 1. At $T=T_C$, the Arrott plot isotherm is *linear* over the entire H/M range and upon extrapolation passes through the origin. With $T_C=56.376$ K, $M(T,0)$ and $\chi^{-1}(T)$ are determined in this way from the Arrott plot, spontaneous magnetization and inverse initial susceptibility are plotted against reduced temperature, $\epsilon=(T-T_C)/T_C$, in Figs. 2 and 3 over a wide temperature range that includes the critical region. By contrast, $\chi_{ac}(T)$, when corrected for demagnetization, is a direct measure of the ''zero-field'' intrinsic susceptibility, $\chi(T)$. Henceforth, $\chi(T)$ data obtained through extrapolation and those measured directly are referred to as $\chi_{dc}(T)$ and $\chi_{ac}(T)$, respectively. With a view to ascertain which of the theories of critical phenomena correctly describes the observed asymptotic critical behavior of weak itinerant ferromagnets, $M(T,0)$, $\chi(T)$, and $M(T_C,H)$, data are analyzed in terms of the following expressions. These expressions exhaust all the theoretical predictions[5–8] relevant to the case under consideration by either including or excluding the leading *multiplicative* logarithmic or *additive* logarithmic/nonanalytic correction to the single power laws.

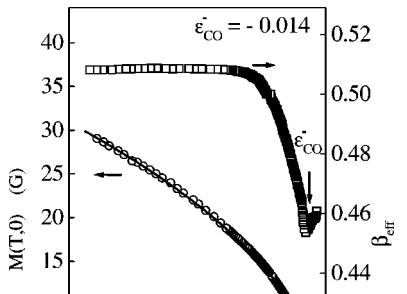

FIG. 2. Temperature variations of the spontaneous magnetization, $M(T,0)$ and its effective critical exponent, β_{eff}. ϵ_{CO}^{-} marks the reduced temperature at which a crossover from asymptotic critical behavior to Gaussian regime begins.

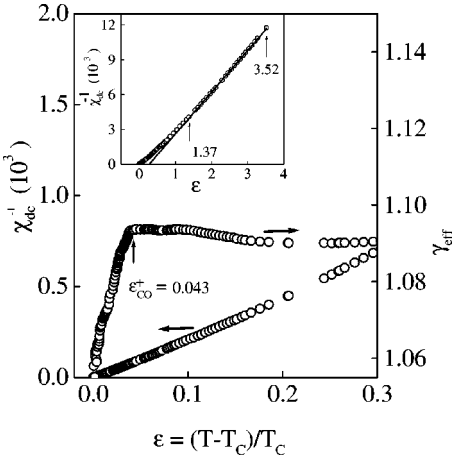

FIG. 3. Temperature variations of the inverse initial dc susceptibility, $\chi_{dc}^{-1}(T)$ and its effective critical exponent, γ_{eff}. ϵ_{CO}^{+} marks the reduced temperature at which a crossover from asymptotic critical behavior to Gaussian regime begins. $\chi_{dc}^{-1}(T)$ is plotted against reduced temperature, ϵ, over a wide temperature range above T_C, in the inset so as to highlight the Curie-Weiss behavior (solid straight line through the data points denoted by open circles) of susceptibility in the reduced temperature range $1.37\lesssim\epsilon\lesssim 3.52$.

$$M(T,0)=B_{eff}(-\epsilon)^{\beta_{eff}}, \qquad \epsilon<0 \tag{1a}$$

$$M(T,0)=B(-\epsilon)^{\beta}|\ln|\epsilon||^{x^-}, \qquad \epsilon<0 \tag{1b}$$

$$M(T,0)=\hat{B}(-\epsilon)^{\beta}[1+\hat{a}_M|\ln|\epsilon||^{x^-}], \qquad \epsilon<0 \tag{1c}$$

$$M(T,0)=B'(-\epsilon)^{\beta}[1+a_M(-\epsilon)^{\Delta_M}], \qquad \epsilon<0 \tag{1d}$$

$$\chi^{-1}(T)=\Gamma_{eff}^{-1}\epsilon^{\gamma_{eff}}, \qquad \epsilon>0 \tag{2a}$$

$$\chi^{-1}(T)=\Gamma^{-1}\epsilon^{\gamma}|\ln|\epsilon||^{-x^+}, \qquad \epsilon>0 \tag{2b}$$

$$\chi^{-1}(T)=\hat{\Gamma}^{-1}\epsilon^{\gamma}[1+\hat{a}_\chi|ln|\epsilon||^{-x^+}]^{-1}, \qquad \epsilon>0 \tag{2c}$$

$$\chi^{-1}(T)=\Gamma'^{-1}\epsilon^{\gamma}[1+a_\chi\epsilon^{\Delta_\chi}]^{-1}, \qquad \epsilon>0 \tag{2d}$$

$$H=D_{eff}M^{\delta_{eff}}, \qquad \epsilon=0 \tag{3a}$$

$$H=DM^{\delta}|\ln|M||^{-\delta x^0}, \qquad \epsilon=0 \tag{3b}$$

$$H=\hat{D}M^{\delta}[1+\hat{a}_H|\ln|M||^{-\delta x^0}], \qquad \epsilon=0 \tag{3c}$$

$$H=D'M^{\delta}[1+a_HM^{\Delta_H}], \qquad \epsilon=0 \tag{3d}$$

In Eqs. (1)–(3), $x^-(\Delta_M)$, $x^0(\Delta_H)$, and $x^+(\Delta_\chi)$ are the exponents of the leading logarithmic (nonanalytic) corrections.

Using the expressions (1a) and (2a), the *effective* critical exponents β_{eff} and γ_{eff}, defined as $\beta_{eff}(\epsilon)=d[\ln M(|\epsilon|)]/d(\ln|\epsilon|)$ and $\gamma_{eff}(\epsilon)=d[\ln\chi^{-1}(\epsilon)]/d(\ln\epsilon)$, are calculated at different temperatures from the $M(\epsilon)$ and $\chi^{-1}(\epsilon)$ data depicted in Figs. 2 and 3. $\beta_{eff}(\epsilon)$ and $\gamma_{eff}(\epsilon)$, so obtained, are also displayed in these figures. In the plots of β_{eff} vs ϵ (Fig. 2) and γ_{eff} vs ϵ (Fig. 3), $\epsilon_{CO}^-=-0.014$ and $\epsilon_{CO}^+=0.043$ mark the temperatures (indicated by downward arrows) at which a crossover from the asymptotic to nonasymptotic critical behavior occurs. Thus the asymptotic critical region spans the temperatures in the ranges $1.77\times10^{-5}\leqslant\epsilon\leqslant1.35\times10^{-2}$ for $M(T,0)$ and $7.0\times10^{-5}\leqslant\epsilon\leqslant4.3\times10^{-2}$ for $\chi_{dc}(T)$. Detailed ''range-of-fit'' analysis[13,14] of the $M(T,0)$, $M(T_C,H)$, and $\chi^{-1}(T)$ data (taken in the asymptotic critical region), based on Eqs. (1)–(3), reveals the following.

(I) Neither the single power laws (SPL), Eqs. (1a) and (2a), nor the expressions, Eqs. (1c)/(1d) and (2c)/(2d), involving the additive logarithmic corrections (ALC)/ nonanalytic corrections (NAC) but *only those*, Eqs. (1b) and (2b), that *include* the leading *multiplicative* logarithmic corrections (MLC) reproduce the observed temperature variations of $M(T,0)$ (Fig. 4) and $\chi_{ac}^{-1}(T)$ or $\chi_{dc}^{-1}(T)$ (Fig. 5) accurately.

(II) By contrast, the MLC fit (depicted in Fig. 6 by the continuous curve) to the critical isotherm, $M(T_C,H)$, based on Eq. (3b), is marginally better than the SPL [ALC, NAC] fit based on Eq. (3a) [Eqs. (3c), (3d)].

(III) When the lower bound $|\epsilon_{min}|$ (M_{min}) of the fit range is kept constant and the upper bound $|\epsilon_{max}|$ (M_{max}) is varied in the ''range-of-fit'' analysis, the parameters corresponding to the SPL/ALC/NAC fits vary *monotonously*

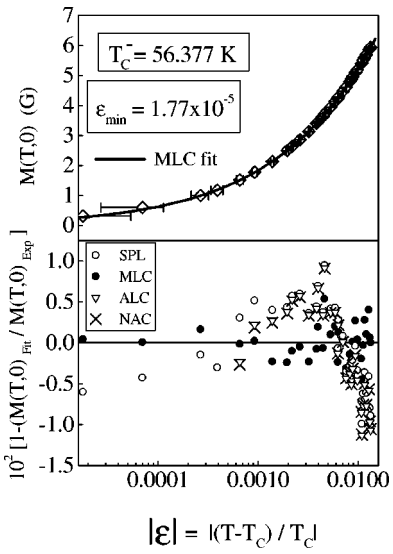

FIG. 4. Spontaneous magnetization, $M(T,0)$ and percentage deviation of $M(T,0)$ data from the best least-squares SPL, MLC, ALC, and NAC fits (see the text for details concerning the different types of fits), based on Eqs. (1a)–(1d), as functions of reduced temperature. The continuous curve through the $M(T,0)$ data (open diamonds) is the optimum MLC fit.

while those associated with the MLC fits remain essentially *unaltered* (within the uncertainty limits) as $|\epsilon_{max}|$ (M_{max}) increases, as is evident from the data presented in Figs. 7–9. Since the parameter variations with $|\epsilon_{max}|$ (M_{max}) are the *same* for the SPL, ALC, and NAC fits, such data for the SPL fits alone are displayed in these figures. Identical parameter variations in the case of SPL, ALC, and NAC fits is a consequence of the fact that the correction amplitudes $\hat{a}_M$, a_M, $\hat{a}_\chi$, a_χ, and $\hat{a}_H$, a_H take on negligibly small values.

Observation (I) is vindicated by the robustness of the fitting parameters against variation in the range of fit (Figs. 7 and 8) and by the result (lower part of Figs. 4 and 5) that the percentage deviation of the $M(T,0)$ and $\chi_{ac}^{-1}(T)$, $\chi_{dc}^{-1}(T)$ data from the best least-squares fits based on Eqs. (1b) and (2b) is *smaller* in magnitude and *evenly* distributed around the theoretically calculated values, whereas the optimum SPL/ALC/NAC fits, based on Eqs. (1a)/(1c)/(1d) and (2a)/(2c)/(2d), present *systematic* deviations from the data so much so that such deviations blow up as $\epsilon\rightarrow0$ [particularly for $\chi^{-1}(T)$; to highlight the departure of the data from the different types of fits in the entire asymptotic critical region, such large deviations are *not shown* in Figs. 4 and 5]. By comparison, the percentage deviation of the $M(T_C,H)$ data from the optimum fits based on Eqs. (3a)–(3d), shown in the lower part of Fig. 6, does not permit a clear-cut distinction between the SPL, MLC, ALC, and NAC fits to be made. However, a slightly lower (by nearly 8%) value of the sum of deviation squares and substantially lower deviations at low fields (Fig. 6) in the case of the MLC fit does tilt the balance in its favor. The *optimum* MLC fits to the $M(T,0)$, $\chi_{ac}^{-1}(T)$, $\chi_{dc}^{-1}(T)$, and $M(T_C,H)$ data are depicted by the *continuous curves* in Figs. 4–6. Based on the variations of the fitting parameters in the asymptotic critical region

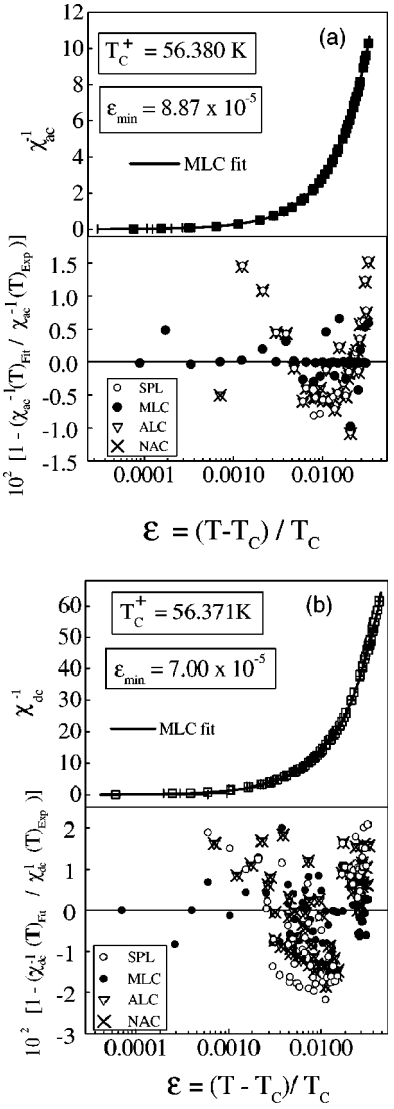

FIG. 5. Inverse initial susceptibility, (a) $\chi_{ac}^{-1}(T)$ or (b) $\chi_{dc}^{-1}(T)$, and percentage deviation of $\chi^{-1}(T) \equiv \chi_{ac}^{-1}(T) or\ \chi_{dc}^{-1}(T)$ data from the best least-squares SPL, MLC, ALC, and NAC fits (see the text for details concerning the different types of fits), based on Eqs. (2a)–(2d), as functions of reduced temperature. The continuous curves through the $\chi_{ac}^{-1}(T)$ (closed squares) and $\chi_{ac}^{-1}(T)$ (open squares) data are the optimum MLC fits.

yielded by the ''range-of-fit'' analysis[13,14] (Figs. 7–9), we arrive at the final values for the quantities of interest listed in Table I. Note that all the independent determinations of the Curie temperature from the $M(T,0)$, $\chi_{ac}^{-1}(T)$, $\chi_{dc}^{-1}(T)$, and $M(T_C,H)$ data yield the *same* value within the uncertainty limits, i.e., $T_C^- = T_C^0 = T_C^+$. This serves as a consistency check. Moreover, magnetization and ac susceptibility measurements performed on different samples of Ni_3Al that have undergone the *same* annealing treatment yield *identical* results.

IV. RESULTS AND DISCUSSION

While mean-field values of the asymptotic critical exponents β, γ, and δ rule out the possibility of an isotropic

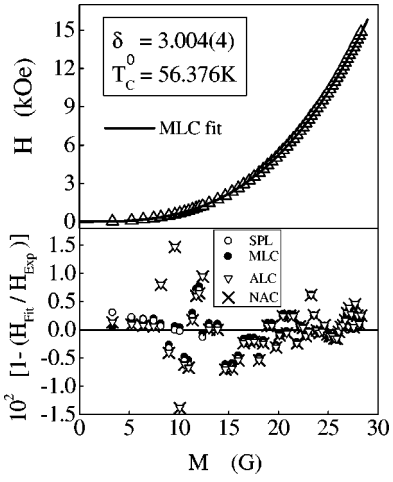

FIG. 6. H versus M isotherm at $T = T_C$. Percentage deviation of $H(M)$ data taken at $T = T_C$ from the best least-squares SPL, MLC, ALC, and NAC fits, based on Eqs. (3a)–(3d) as a function of M. The continuous curve through the $H(M)$ data (open triangles) is the optimum MLC fit.

Heisenberg or isotropic dipolar critical behavior in Ni_3Al, the logarithmic corrections to mean-field power laws seem to suggest that Ni_3Al may belong to one of those universality classes for which the renormalization group (RG) theories predict such corrections. These classes are: (a) systems with[15,16] spin dimensionality, n and space dimensionality, $d=4$, (b) *uniaxial* dipolar ferromagnets[6] with $d=3$ and $n=1$, (c) *isotropic* d-dimensional ferromagnets with n-component spins and long-range interactions between spins decaying[7] as $J(r) \sim 1/r^{(3/2)d}$, and (d) same as (c) but with[8] $n \to \infty$ (spherical model). One immediately notices that

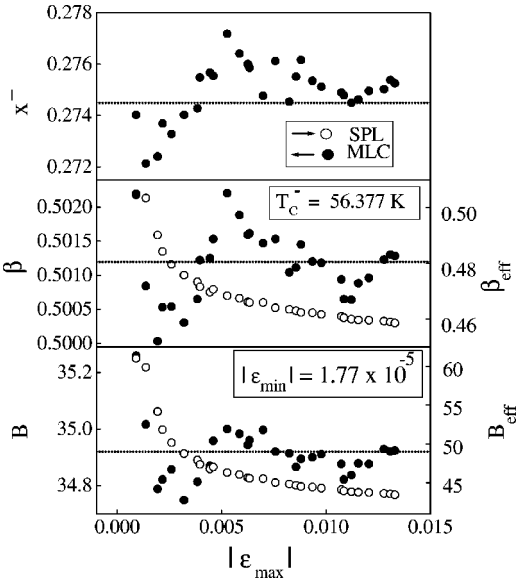

FIG. 7. Variations of the free-fitting parameters with $|\epsilon_{max}|$ in the ''range-of-fit'' analysis of $M(T,0)$ data, using Eqs. (1a) and (1b) of the text. Note the *extreme sensitivity* of the ordinate scales for the parameters B, β, and x^-, and the horizontal dashed lines give their average values.

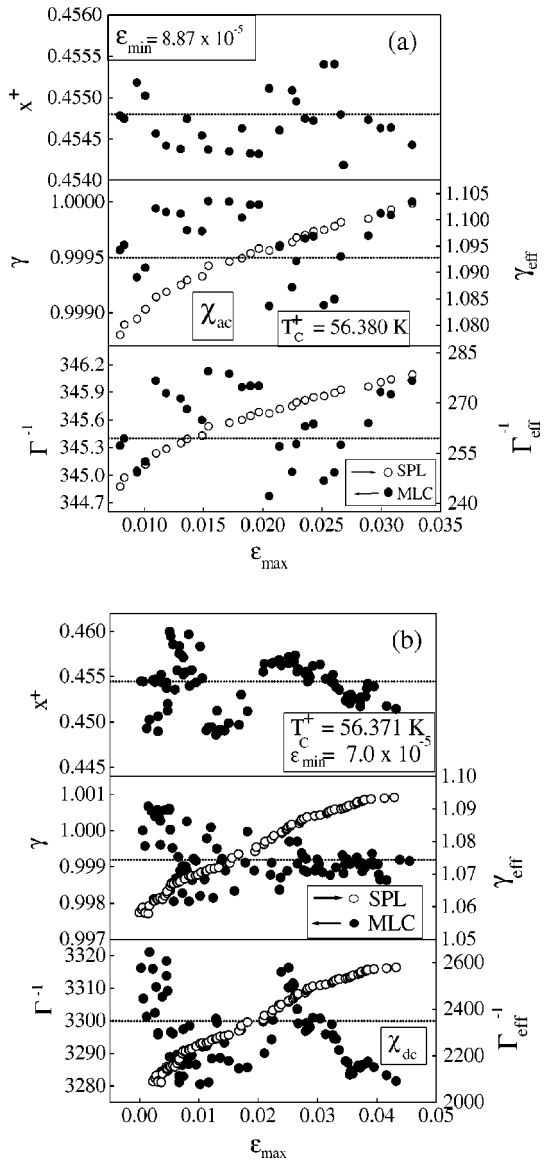

FIG. 8. Variations of the free-fitting parameters with $|\epsilon_{max}|$ in the ''range-of-fit'' analysis of (a) $\chi_{ac}^{-1}(T)$ and (b) $\chi_{dc}^{-1}(T)$ data, using Eqs. (2a) and (2b) of the text. Note the *extreme sensitivity* of the ordinate scales for the parameters Γ^{-1}, γ, and x^+ and the horizontal-dashed lines give their average values.

the universality classes (a) and (d) are not applicable to the three-dimensional ferromagnet in question. The presently determined values of the exponents x^-, x^+, and x^0 of the logarithmic correction terms, defined by the Eqs. (1b), (2b), and (3b), as well as the universal amplitude ratio R_χ are compared with the corresponding theoretical estimates[6,7] specific to each of the universality classes (b) and (c), in Table I. From such a comparison between theory and experiment, it is evident that the values x^-, x^+, x^0, and R_χ determined in this work are completely different from those predicted by theory for a $d=3$ uniaxial-dipolar ferromagnet. By contrast, the RG calculations for $d=3$, $n=3$ isotropic ferromagnet in which the interaction between spins decays as $J(r)\sim 1/r^{(3/2)d}$ yield the estimates for the exponents x^- and x^+ that are in very good agreement with the experimental

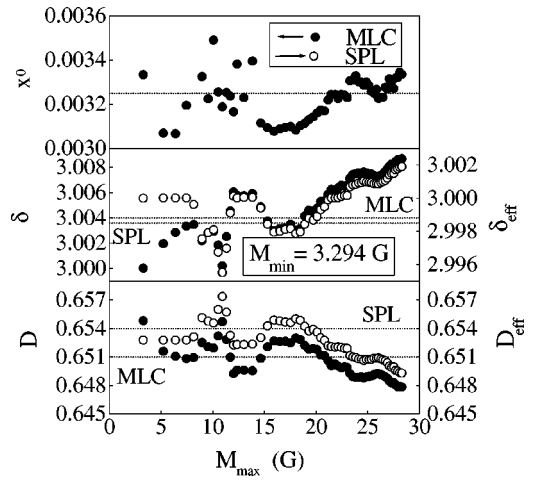

FIG. 9. Variations of the free fitting parameters with M_{max} in the ''range-of-fit'' analysis of $H(M)$ data taken at $T=T_C$ using Eqs. (3a) and (3b) of the text. The horizontal-dashed lines give the average values of the SPL and MLC fit parameters.

values. However, in the absence of the theoretical estimates for the quantities x^0 and R_χ no definite conclusion can be drawn from this agreement.

Having established the existence of multiplicative logarithmic corrections to mean-field power laws in the asymptotic critical region, an attempt is made to ascertain the magnetic behavior of Ni_3Al outside this region. The ''range-of-fit'' analysis of $M(T,0)$ and $\chi_{dc}^{-1}(T)$ data taken at temperatures outside the asymptotic critical region, based on Eqs. (1) and (2), reveals that the optimum fits (continuous curves) based on the expressions (1d) and (2d), which include the corrections to mean-field (MF) leading exponents arising from Gaussian fluctuations, with $B'=50.0(3)$ G, $\beta=0.500(8)$, $a_M=0.08(2)$ (in the temperature range 31.93 K$\leqslant T\leqslant$41.73 K), $\Gamma'^{-1}=3065(145)$, $\gamma=0.995(5)$, $a_\chi=0.025(2)$ (in the temperature interval 70.11 K$\leqslant$T$\leqslant$93.75 K), $T_C^{MF^-}=T_C^{MF^+}=59.8(2)$ K, and $\Delta_M=\Delta_\chi$ *fixed* at 1.0, as expected for the Gaussian fixed point, describe the data *better* than the pure mean-field power laws (dashed lines), Eqs. (1a) and (2a) with $\beta_{eff}=0.5$ and $\gamma_{eff}=1.0$, at temperatures that lie well below and above the Curie temperature (Fig. 10). The correction due to Gaussian fluctuations turns out to be more important in the ferromagnetic regime than in the paramagnetic regime. In order to bring out this observation clearly, β_{eff} and γ_{eff} are plotted against the reduced temperature $\epsilon^{MF}=(T-T_C^{MF})/T_C^{MF}$ in the above mentioned temperature ranges (indicated by upward arrows in Fig. 10), i.e., $-0.47\leqslant\epsilon^{MF}\leqslant-0.30$ and $0.18\leqslant\epsilon^{MF}\leqslant0.58$, in Fig. 11. The straight-line fits through the $\beta_{eff}(\epsilon^{MF})$ and $\gamma_{eff}(\epsilon^{MF})$ data points (open circles) are based on the expressions

$$\beta_{eff}(\epsilon^{MF})=\beta+a_M\Delta_M(-\epsilon^{MF})^{\Delta_M} \tag{4}$$

and

$$\gamma_{eff}(\epsilon^{MF})=\gamma+a_\chi\Delta_\chi(\epsilon^{MF})^{\Delta_\chi} \tag{5}$$

TABLE I. Comparison between experiment and theory.

Parameters	Method	Experiment	Theory		
		Ni_3Al	$d=3,\ n=3$ $J(r)\sim r^{-(3/2)d}$ (Ref. 7)	$d=3,\ n=1$ Uniaxial dipolar (Ref. 6)	Mean field (Ref. 16)
T_C^- (K)	$M(T,0)$/LC	56.377(5)			
B_{eff}	$M(T,0)$/SPL	35.0(3)			
β_{eff}	$M(T,0)$/SPL	0.48(2)			
B	$M(T,0)$/LC	34.9(2)			
β	$M(T,0)$/LC	0.501(1)	0.5	0.5	0.5
x^-	$M(T,0)$/LC	0.2745(25)	3/11	1/3	
Fit range in $\epsilon(10^{-4})$ for above parameters		0.18–133			
T_C^+ (K)	χ_{dc}/LC	56.371(5)			
	χ_{ac}/LC	56.380(5)			
Γ_{eff}^{-1}	χ_{dc}/SPL	2315(212)			
	χ_{ac}/SPL	262(17)			
γ_{eff}	χ_{dc}/SPL	1.075(20)			
	χ_{ac}/SPL	1.092(12)			
Γ^{-1}	χ_{dc}/LC	3300(20)			
	χ_{ac}/LC	345(1)			
γ	χ_{dc}/LC	0.9992(10)	1.0	1.0	1.0
	χ_{ac}/LC	0.9995(5)			
x^+	χ_{dc}/LC	0.4545(55)	5/11	1/3	
	χ_{ac}/LC	0.4548(6)			
Fit range in ϵ (10^{-4})	χ_{dc}	0.7–433			
for above parameters	χ_{ac}	0.89–327			
T_C^0 (K)	$M(T=T_C,H)$/LC	56.376(5)			
D_{eff}	$M(T=T_C,H)$/SPL	0.654(4)			
δ_{eff}	$M(T=T_C,H)$/SPL	2.9985(35)			
D	$M(T=T_C,H)$/LC	0.651(4)			
δ	$M(T=T_C,H)$/LC	3.004(4)	3.0	3.0	3.0
x^0	$M(T=T_C,H)$/LC	0.0033(3)		1/3	
Fit range in $M(G)$ for above parameters		3.2–28.2			
R_χ		0.25(1)		0.5	1.0
$m_0/M(0,0)$		0.75(1)			1.73
$\mu_0 h_0/k_B T_C$		0.0079(1)			1.73
$\beta+\gamma$		1.501(2)	1.5	1.5	1.5
$\beta\delta$		1.505(5)	1.5	1.5	1.5

that relate the *effective* $(\beta_{eff},\gamma_{eff})$ and *asymptotic* (β,γ) critical exponents, defined by Eqs. (1a), (2a) and Eqs. (1d), (2d), respectively. Note that $\beta=\lim_{\epsilon^{MF}\to 0}\beta_{eff}(\epsilon^{MF})$ $[\gamma=\lim_{\epsilon^{MF}\to 0}\gamma_{eff}(\epsilon^{MF})]$ and if $\Delta_M=\Delta_\chi=1$, β_{eff} vs ϵ^{MF} and γ_{eff} vs ϵ^{MF} plots are *straight lines* with slopes (intercepts on β_{eff} and γ_{eff} axes) a_M and a_χ (β and γ), respectively. That this is indeed the case in specific temperature ranges below and above T_C^{MF} is demonstrated by the data presented in Fig. 11. The values of β, a_M, γ, and a_χ deduced from the linear $\beta_{eff}(\epsilon^{MF})$ and $\gamma_{eff}(\epsilon^{MF})$ plots serve as a cross check for those (stated earlier in the text) obtained from the optimum fits (continuous curves in Fig. 10) to the $M(T,0)$ and $\chi^{-1}(T)$ data based on Eqs. (1d) and (2d). Another important point to note is that if the Gaussian corrections were not important, β_{eff} and γ_{eff} would have had constant values $\beta=0.5$ and $\gamma=1.0$ regardless of the value of ϵ^{MF} within the temperature ranges in question. Finite slopes of the $\beta_{eff}(\epsilon^{MF})$ and $\gamma_{eff}(\epsilon^{MF})$ linear plots (Fig. 11) therefore assert that the Gaussian corrections are significant. Furthermore, it is evident from the temperature variations of β_{eff} and γ_{eff}, shown in Figs. 2 and 3, and from the $[M(T,0)]^2$ and $\chi^{-1}(T)$ data displayed in Fig. 10, that a crossover from the asymptotic critical behavior, characterized by multiplicative logarithmic corrections to mean-field power laws, to the Gaussian fixed point does not occur abruptly at a certain well-defined temperature but gradually over a fairly wide temperature range.

In order to arrive at a possible theoretical description, we address the issue of why Ni_3Al exhibits an asymptotic critical behavior that is characterized by mean-field power laws with logarithmic corrections. Obviously, the answer to this question should lie in the symmetry of the Hamiltonian

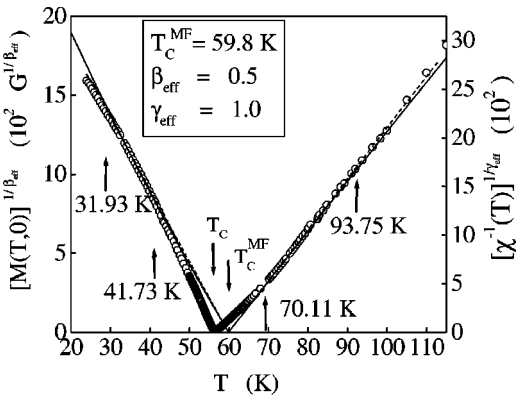

FIG. 10. In order to highlight the importance of the corrections to the mean-field behavior arising from Gaussian fluctuations, the quantities $[M(T,0)]^{1/\beta_{eff}}$ and $[\chi^{-1}(T)]^{1/\gamma_{eff}}$ with the mean field choice ($\beta_{eff}=0.5$ and $\gamma_{eff}=1.0$) of the exponents β_{eff} and γ_{eff} are plotted against temperature. The best least-squares mean-field and Gaussian fits to the data, based on Eqs. (1a), (2a) and (1d), (2d) of the text, are depicted by the dashed straight lines and solid curves, respectively. If the Gaussian corrections are not important, such plots should be *linear* (dashed straight lines) over the temperature intervals marked by the upward arrows below and above the mean-field Curie temperature, T_C^{MF}.

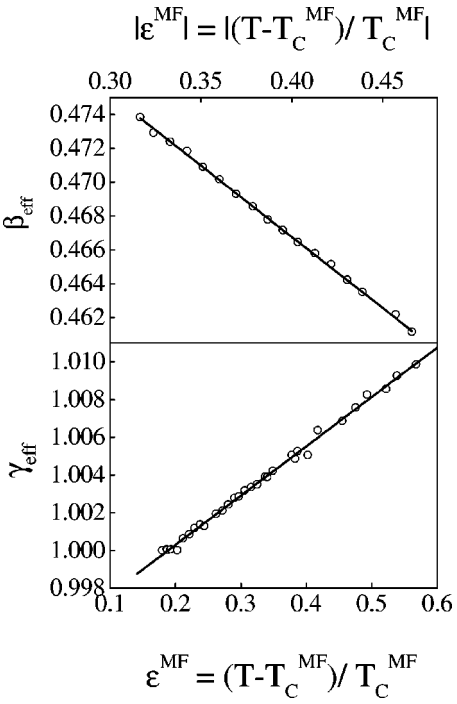

FIG. 11. Effective critical exponents β_{eff} and γ_{eff} plotted against the reduced temperature, $\epsilon^{MF}=(T-T_C^{MF})/T_C^{MF}$, referred to the Gaussian fixed point critical temperature T_C^{MF}. The straight lines through the data points (open circles) represent the best least-squares fits based on the Eqs. (4) and (5) of the text.

and/or the range of interaction. To this end, the following observations merit serious consideration. A detailed investigation[17] of magnetocrystalline anisotropy in the weak itinerant ferromagnet Ni_3Al has revealed the following. (i) Ni_3Al, like pure Ni, exhibits a *cubic* magnetocrystalline anisotropy in the ferromagnetic regime with [111] crystal direction as the preferred orientation of magnetization. (ii) The *leading* anisotropy constant K_1 is about *two orders of magnitude smaller* than in pure Ni at 4.2 K. (iii) As in crystalline Ni, K_1 in Ni_3Al is *negative* and decreases in magnitude very rapidly with increasing temperature and *vanishes* as the Curie temperature is approached from below. In view of these findings, Ni_3Al is expected to behave as an *isotropic* spin system in the asymptotic critical region. It is well known that the ratio of the spin-wave stiffness D to the Curie temperature T_C is a *direct* measure of the range of interaction in the localized-electron model. The value $(D/T_C)=1.25(1)(\text{meV\AA}^2)\,\text{K}^{-1}$ reported[12,18] for Ni_3Al, when compared with the estimate $(D/T_C)=0.144\ \text{meV\AA}^2\text{K}^{-1}$ predicted[19] by the nearest-neighbor Heisenberg model, asserts that the interactions coupling the magnetic moments in Ni_3Al are of *long-range* type. The $\chi^{-1}(T)$ data, displayed in the inset of Fig. 3, follow the Curie-Weiss behavior in the temperature range $1.37\leqslant\epsilon\leqslant3.52$. The inverse slope of the straight-line fit, based on the Curie-Weiss law, yields the Curie constant C, which, in turn, permits an accurate determination of the effective atomic moment in the paramagnetic state, q_C, through the relation $q_C(q_C+2)=(2.828)^2\ CA/\rho$, where A and ρ are the atomic weight and density, respectively. From the value $q_C=0.358(1)\ \mu_B$, so obtained, and the estimate $q_S=0.0575(1)\ \mu_B$ for the magnetic moment per alloy atom at 0 K for the *same*-sample reported[12] earlier, q_C/q_S ratio turns out to be 6.23(2), as against $(q_C/q_S)=1.0$, which is the case when magnetic moments are *localized* at the lattice sites. According to the Rhodes-Wohlfarth criterion,[20] the greater the amount by which the q_C/q_S ratio exceeds unity, the more *itinerant* are the magnetic moments. Thus, the localized moment picture cannot form a correct theoretical description of the magnetism in Ni_3Al. It immediately follows that the long-range interactions such as the dipole-dipole and the Ruderman-Kittel-Kasuya-Yosida interactions are not relevant to the case under consideration. Even otherwise, the dipole-dipole interactions, which are proportional to the magnetic-moment *squared*, are expected to be extremely weak in Ni_3Al due to the small magnitude of q_S (an order of magnitude smaller than in crystalline Ni).

Above considerations, the observation of logarithmic corrections to the mean-field power laws and a close agreement between the values $x^-=0.2745(25)$, $x^+=0.4545(55)$, and those ($x^-=3/11$, $x^+=5/11$) characterizing the asymptotic critical behavior of an *isotropic* $d=3$, $n=3$ ferromagnet in which long-range interactions between spins decay[7] with distance (r) as $J(r)\sim1/r^{(3/2)d}$ (Table I), completely rule out the possibility of an isotropic short-range Heisenberg or an isotropic long-range dipolar or a uniaxial dipolar asymptotic critical behavior in Ni_3Al. They do, however, indicate that the weak itinerant ferromagnet Ni_3Al may be a potential candidate for the universality class for critical-point phenomena represented by the special case, $d=3$, $n=3$, and $\sigma=d/2$ in the power law, $J(r)\sim1/r^{d+\sigma}$, dependence of the intermoment interaction on distance, of the renormalization group calculations[7] on an *isotropic* ferromagnet with space dimen-

sionality d, spin dimensionality n, and long-range attractive interactions between spins of the above form. That the RG treatment due to Fisher *et al.*[7] also describes correctly the asymptotic critical behavior of the strong itinerant ferromagnet Ni, has been demonstrated[21] recently.

V. SUMMARY AND CONCLUSION

High-precision magnetization and ac (''zero-field'') susceptibility measurements have been performed on several annealed polycrystalline samples of Ni_3Al with long-range atomic order parameter of 0.55(3) over a wide range of temperatures. A detailed analysis of the data, so obtained, reveal the existence of multiplicative logarithmic corrections to the mean-field power laws in the asymptotic critical region and a gradual crossover to the Gaussian fixed point at temperatures outside the critical regime, irrespective of the choice of samples. The correction to the mean-field behavior due to Gaussian fluctuations is found to be more important in the ferromagnetic regime than the paramagnetic regime. First accurate determination of the amplitude ratio $R_\chi = DB^{\delta-1}\Gamma$, the asymptotic critical exponents β, γ, and δ, and the logarithmic correction exponents x^-, x^+, and $x°$ for the spontaneous magnetization, initial susceptibility and the magnetization vs field isotherm at the Curie temperature T_C, coupled with the vanishingly small, or even no, magnetocrystalline anisotropy in the asymptotic critical region and the extremely large magnitudes of the ratios D/T_C and q_C/q_S permits us to completely rule out the possibility of an isotropic short-range Heisenberg or an isotropic long-range dipolar or a uniaxial dipolar asymptotic critical behavior in Ni_3Al. These observations, instead, strongly suggest that in the asymptotic critical regime the weak itinerant ferromagnet Ni_3Al behaves as an *isotropic* $d=3$, $n=3$ ferromagnet in which the attractive interactions between magnetic moments decay with distance (r) as $J(r) \sim 1/r^{(3/2)d}$. However, in the absence of the theoretical estimates for the universal amplitude ratio R_χ and the logarithmic correction exponent $x°$, this analogy has to be treated with caution. Detailed RG calculations are needed to clinch this issue.

ACKNOWLEDGMENTS

This work was supported by the Department of Science and Technology, India, under the Grant D.O. No. SP/S2/M-21/97. A.S. gratefully acknowledges the financial support received from the Council of Scientific and Industrial Research, India.

*Author to whom correspondence should be addressed. Email address: kaulsp@uohyd.ernet.in

[1] S.N. Kaull, J. Phys.: Condens. Matter **11**, 7597 (1999), and references therein.
[2] T. Moriya, *Spin Fluctuations in Itinerant Electron Magnetism* (Springer, Berlin, 1985).
[3] G.G. Lonzarich and L. Taillefer, J. Phys. C **18**, 4339 (1985).
[4] Y. Takahashi, J. Phys. Soc. Jpn. **55**, 3553 (1986).
[5] A. Aharony and M.E. Fisher, Phys. Rev. B **8**, 3323 (1973); A.D. Bruce and A. Aharony, *ibid.* **10**, 2078 (1974); A.D. Bruce J. Phys. C **10**, 419 (1977); E. Frey and F. Schwabl, Phys. Rev. B **43**, 833 (1991).
[6] A.I. Larkin and D.E. Khmel'nitskii, Zh. Éksp. Teor. Fiz. **56**, 2087 (1969) [Sov. Phys. JETP **29**, 1123 (1969)]; A. Aharony, Phys. Rev. B **8**, 3363 (1973); E. Brézin, and J. Zinn-Justin, *ibid.* **13**, 251 (1976); E. Frey and F. Schwabl, *ibid.* **42**, 8261 (1990); K. Ried, Y. Millev, M. Fähnle, and H. Kronmüller, *ibid.* **51**, 15 229 (1995).
[7] M.E. Fisher, S.K. Ma, and B.G. Nickel, Phys. Rev. Lett. **29**, 917 (1972); J. Sak, Phys. Rev. B **8**, 281 (1973).
[8] G.S. Joyce, Phys. Rev. **146**, 349 (1966).
[9] J.S. Kouvel and J.B. Cowly, in *Critical Phenomena in Alloys, Magnets and Superconductors*, edited by R.E. Mills, E. Ascher, and R.I. Jaffee (McGraw-Hill, New York, 1971) p. 437; R. Jesser, A. Bieber, and R. Kuentzler, J. Phys. (Paris) **44**, 631 (1983).
[10] Y. Shen, I. Nakai, H. Maruyama, and O. Yamada, J. Phys. Soc. Jpn. **54**, 3915 (1985); M. Seeger and H. Kronmüller, J. Magn. Magn. Mater. **78**, 393 (1989); O. Boxberg and K. Westerholt, Phys. Rev. B **50**, 9331 (1994).
[11] M. Seeger, H. Kronmüller, and H.J. Blythe, J. Magn. Magn. Mater. **139**, 312 (1995).
[12] A. Semwal and S.N. Kaul, Phys. Rev. B **60**, 12 799 (1999).
[13] S. Srinath, S.N. Kaul, and H. Kronmüller, Phys. Rev. B **59**, 1145 (1999); S. Srinath and S.N. Kaul, *ibid.* **60**, 12 166 (1999).
[14] S.N. Kaul, Phys. Rev. B **38**, 9178 (1988); S.N. Kaul and M. Sambasiva Rao, *ibid.* **43**, 11 240 (1991).
[15] F.J. Wegner and E.K. Riedel, Phys. Rev. B **7**, 248 (1973); E. Brézin, J. Phys. (Paris) **36**, L51 (1975).
[16] S.N. Kaul, J. Magn. Magn. Mater. **53**, 5 (1985).
[17] T.I. Sigfusson and G.G. Lonzarich, Phys. Scr. **25**, 720 (1982).
[18] F. Semadeni, B. Roessli, P. Böni, P. Vorderwisch, and T. Chatterji, Phys. Rev. B **62**, 1083 (2000).
[19] S.N. Kaul, Phys. Rev. B **27**, 5761 (1983).
[20] E.P. Wohlfarth, J. Magn. Magn. Mater. **7**, 113 (1978).
[21] M. Seeger, S.N. Kaul, H. Kronmüller, and R. Reisser, Phys. Rev. B **51**, 12 585 (1995).